

Presented at the First International Conf. on Large Scale
Applications and Radiation Hardness of Semiconductor
Detectors, Italy, July 7-9, 1993

BNL-49823

RECEIVED

FEB 04 1994

OSTI

Ionizing Radiation Effects on Silicon Test Structures*

H. W. Kraner, R. Beuttenmuller, W. Chen, Lie Dou^o, E. Fretwurst⁺, G. Lindstroem⁺,
J. A. Kierstead, Z. Li and Y. Zhang

Brookhaven National Laboratory
University of Hamburg⁺, Germany
Wayne State University^o

December 1993

*This research was supported by the U.S. Department of Energy:
Contract No. DE-AC02-76CH00016.

MASTER

2B

IONIZING RADIATION EFFECTS ON SILICON TEST STRUCTURES

H. W. Kraner, R. Beuttenmuller, W. Chen, Lie Dou °, E. Fretwurst*,
J. A. Kierstead, G. Lindstroem+, Z. Li and Y. Zhang

Brookhaven National Laboratory
University of Hamburg+, Germany
Wayne State University°

Abstract

The effects of ^{60}Co gamma irradiation on MOSCAPS and special junction diode detectors have been studied. The capacitors were used to elicit the charge accumulation and anneal in two types of thermally grown oxides representative of those used in routine detector processing. Ion implanted, oxide passivated junction detectors having 0.25 and 1 cm² areas and perimeter to area ratios of 1 (a square), 2 and 5 were designed and constructed to amplify the ionizing effects expected to largely affect junction edges through changes in fixed oxide charges. Detectors were exposed to over 4Mrad and showed clear increases in leakage current in proportion to the junction edge length. Annealing schedules were determined to provide a continuous response to incremental irradiations and subsequent room temperature anneals of leakage current. Besides an increase in gate threshold, little effect on the C(V) response was found. PISCES simulation of the edge fields using different fixed oxide charge revealed regions of very high lateral fields near the junction edges for fixed charges in the $2 \times 10^{12}/\text{cm}^2$ range expected from the capacitor studies which could be responsible for the observed leakage currents.

Introduction

It is expected that the electrical effects of ionizing radiation on silicon planar passivated junction detectors will involve the junction edges and result from changes in the electric fields nearby from charges generated in the oxide. It is improbable but not impossible that Compton or secondary electrons from the radiation would generate displacement defects (if the kinematic limit of $E > 160\text{KeV}$ is exceeded), but these effects will not be emphasized. It is well known [1,2] that ionizing radiation in the silicon dioxide passivating layer produces residual positive charge primarily if an electric field is applied during the irradiation. This positive charge consists schematically of fixed charge in the bulk SiO₂, somewhat mobile charge in the bulk SiO₂ and charged and neutral interface states at the Si-SiO₂ interface. A positive gate bias greatly enhances the amount of total charge, Q_{SS}, as holes are driven to the interface and both reside on interface states and contribute to their creation [3]. Electrons are highly mobile in the SiO₂ but holes do retain a sufficient mobility for movement under the

applied fields [2]. However, a negative gate (the contact electrode as it overlaps the edge oxide) bias will also result in significant addition of positive charge, perhaps SiO₂ bulk charge, even though most of the holes are collected at the gate electrode. It is this latter condition that one finds at the junction edge of p⁺-n diode structures with metallization that commonly overlaps the oxide edge to act as a field plate, dispersing the intrinsic positive interface charge.

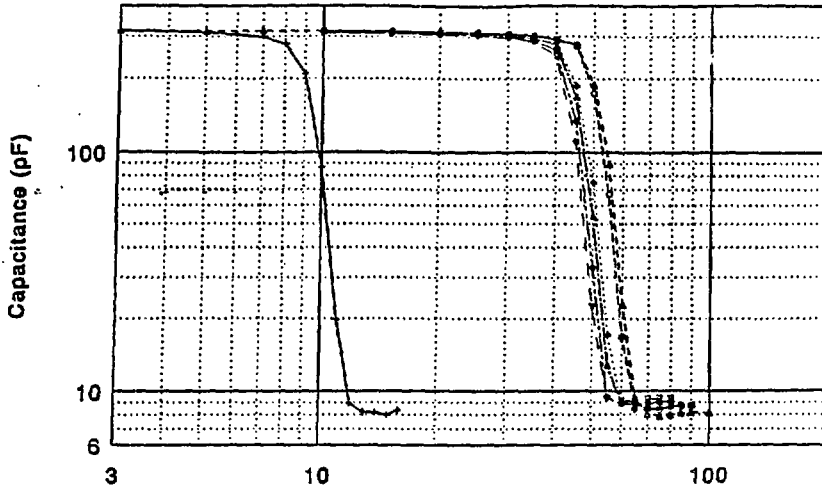
The deleterious effects of ionizing radiation that might be expected will result from the increase and perhaps "rearrangement" of the oxide charge and its affect on the edge electric fields. New defect states at the interface which add surface current are also expected [1] and edge leakage currents will most certainly increase. In this work, a study is presented on the oxide charge changes observed in typical "detector" oxides with MOS capacitors on test wafers; the current and capacitive effects on test structures with variable edge to area ratios and finally the results of PISCES edge electric field simulations will be shown. All irradiations were carried out in air with a calibrated 15kCi ⁶⁰Co source; the rad doses referred to are indeed those of the LiF thermoluminescent dosimeters which read a few per cent lower than Si [1], a relatively minor correction.

MOSCAP Studies

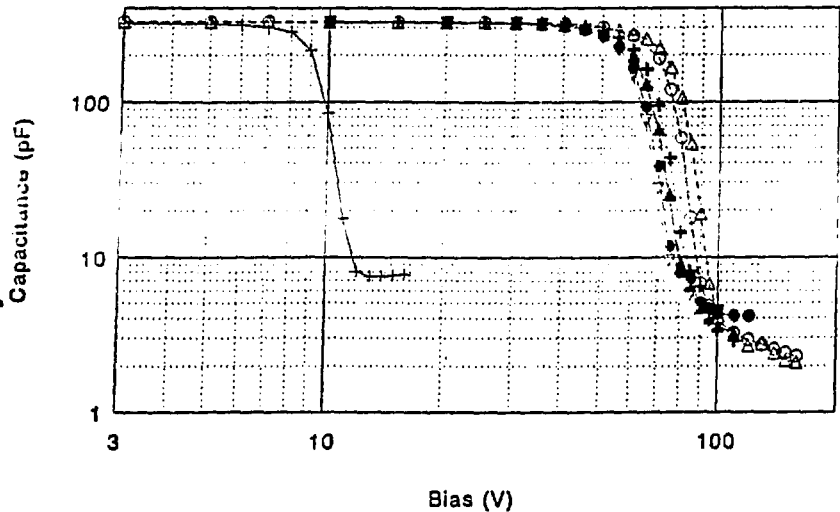
Two and four mm diameter aluminum dots on test wafer pieces were evaporated to form the gate contact of a capacitor with the opposite contact being a large area aluminum evaporation on the silicon itself. Capacitance measurements at 100KHz as a function of bias elicited the flat band voltage (V_{fb}) condition in the transition from accumulation of the n-type base material to its depletion condition. At V_{fb} , $Q_{ss} = C_{ox} V_{fb}$ and C_{ox} is just the geometrical capacity of the oxide using a thickness derived from etch-back studies with oxide colors and the expected SiO₂ dielectric coefficient, 3.9. The results shown below resulted from only 100Krad exposures, however because the oxides are in no way "hardened", very distinct results are observed. Two growth conditions for oxides were used. The first is a relatively standard, type "A" oxide, which is a 18 hr 975C oxidation in dry oxygen after a precondition of the tube at 1200C in 2% TCA for chlorine cleaning; a 2700A thick oxide results. The other is a type "C" oxide [4] which is a longer term oxidation with three temperature stages to promote internal gettering [6], 1100 C, 700C and 1000C with TCA and finally N₂ atmospheres giving a 4700-5000A thick oxide.

Figure 1 shows the C(V) measurements on the A oxides with both positive and negative bias with flat band shifts of approximately 90 and 70 volts resulting from the irradiation with very little recovery over a 9900min period, about one week. Although it is not so evident in log plots, some "stretchout" (DV, between 10-90% of C_{ox} , indicating the contribution of charges in the interface) is observed, especially in the positive bias case as expected. Figure 2 shows the C(V) curves from the C oxide which show even larger flat band shifts due to the amplification by the increased oxide thickness. To assess the scale, a 4700A thick oxide with $Q_{ss} = 10^{12}/cm^2$ will give a 20V flat band shift. Total oxide charge in both oxides, then reside in the mid $10^{12}/cm^2$ range, with both positive and negative biases. Figure 3 shows the C(V) results from MOSCAPS irradiated without bias. Because most of the bulk charge recombines, the only effect is a rather small degree of stretchout due to the creation of interface states from locally produced ionization. Although the effect of positive bias can be easily understood as holes are driven to the interface [6], the effects of negative bias also produce interface defects which have been studied by Jeppson and Svensson [7].

CV MOSCAP 100Krad Gamma Oxide A Negative Bias



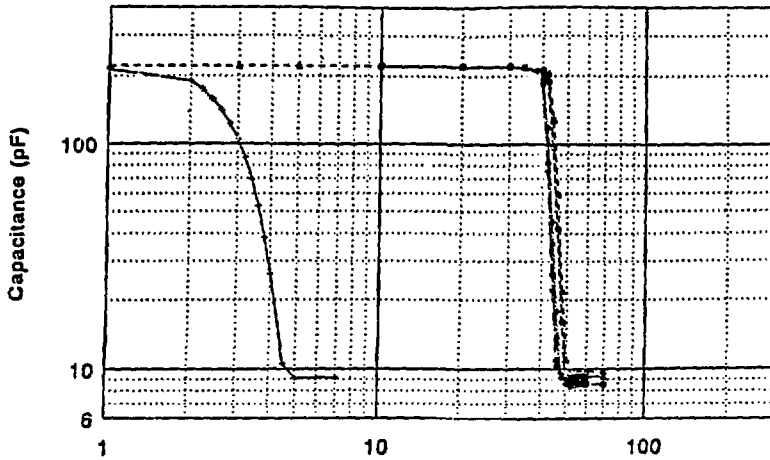
Oxide A Positive Bias



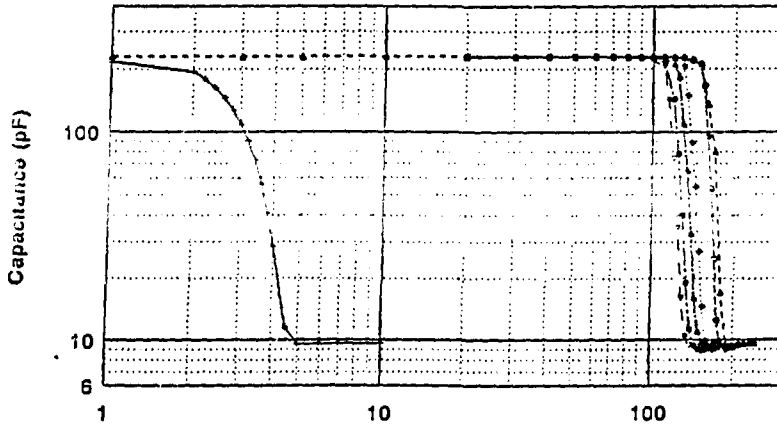
—+— Pre
--Δ-- Post
--○-- 1.3hr
---+--- 17.6hr
--▲-- 43hr
--●-- 3.8d
--▽-- 6.9d

Figure 1. Capacitance vs Bias for MOS Capacitors on the A oxide irradiated under positive and negative bias.

CV MOSCAP 100Krad Gamma Oxide C Negative Bias



Oxide C Positive Bias

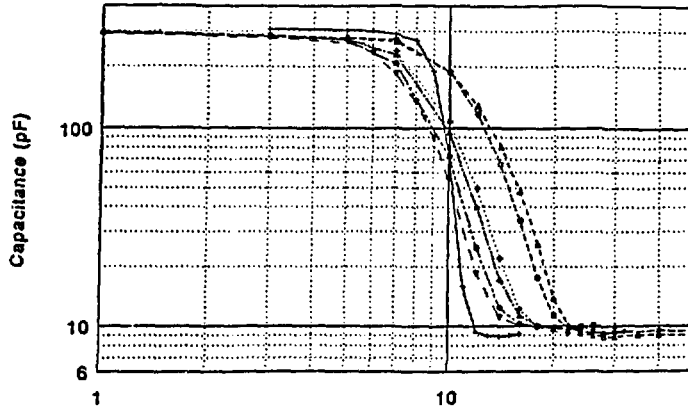


Bias (V)

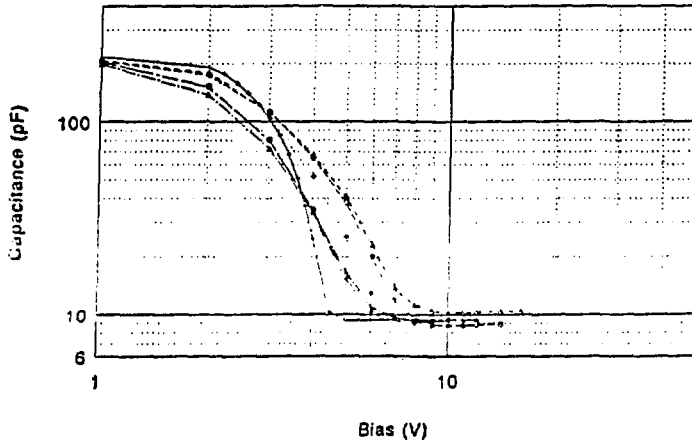
—+— Pre -Δ- Post -○- 1.3hr -+ - 17.6hr
 -▲- 43hr -●- 3.8d -▽- 6.9d

Figure 2. Capacitance vs Bias for MOS Capacitors on the C oxide irradiated under positive and negative bias.

CV MOSCAP 100Krad Gamma Oxide A Unbiased



Oxide C No Bias



Bias (V)

—+— Pre Irrad --Δ-- Post 100 --○-- 1.5hr --+-- 17.6hr
 --▲-- 1.8d --●-- 3.8d --▽-- 6.9d

Figure 3. Capacitance vs Bias for MOS capacitors on A oxide and C oxide irradiated without bias.

The room temperature anneal of the flat band voltage is relatively slow and can best be fitted to a $\ln(\text{time})$ dependence, shown in Figure 4. The upper figure shows the anneal on a linear time scale which emphasizes the short term anneal in the C oxide, which will be discussed in detail later as being due to a greater possibility for Q_{SS} reduction by electron tunneling. Others have observed this time dependence [8,9,14] which has been explained by a systems approach [9] without a direct physical connection. This plot shows quantitatively the values of flat band voltage for each oxide.

Vflat band vs time MOSCAPS A and C oxides, 100Krad

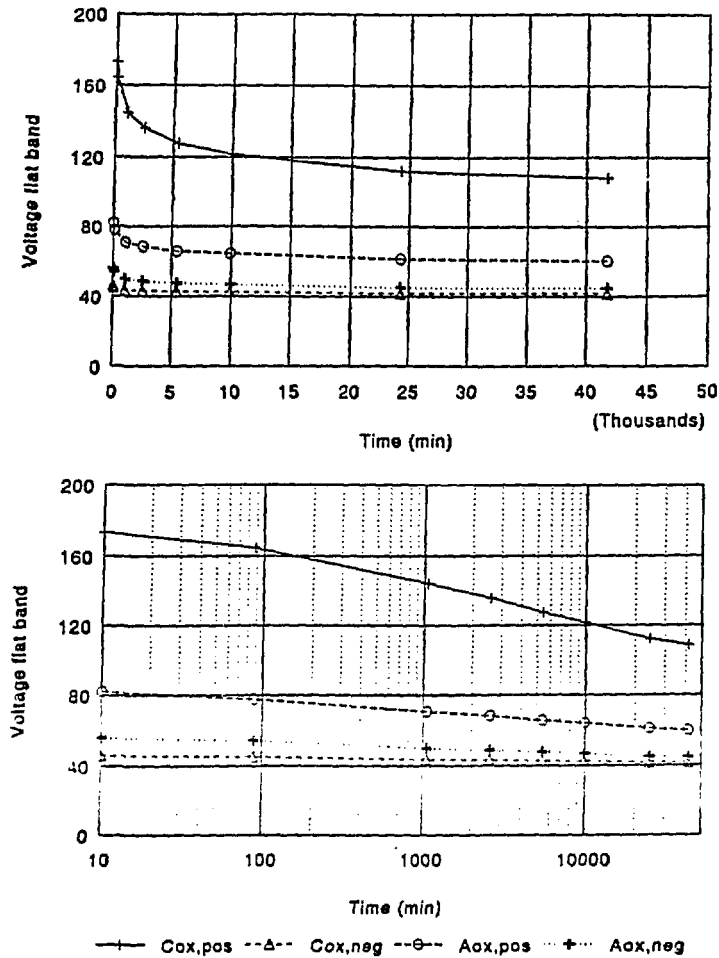
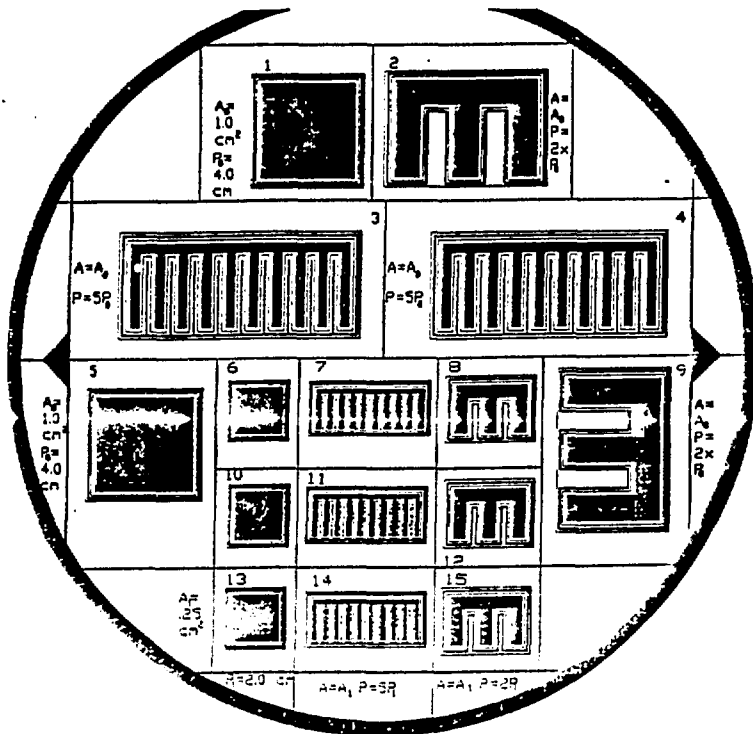


Figure 4. The room temperature anneal of the Flat Band Voltage as function of time after the 100 Krad irradiation.

Detector Test Structure Results

A wafer was designed with detectors having different ratios of perimeter or junction edge to detector area as well as having two different detector areas; it is shown in Figure 5. The "three fingers" design yields twice the perimeter as the square and the multiple fingered unit is five times the perimeter of the square (sometimes referred to inaccurately as the "five-

"fingered" detector). The smaller-sized detectors are 0.25cm^2 and the larger are 1cm^2 . Detectors were fabricated on $5000\Omega\text{-cm}$ n-type (1,1,1) silicon with boron implanted p^+ junctions on 3" wafers, 300mm thick. The passivating oxide was 4700-5000Å thick, "C"-type oxide, basically unhardened. The metallization overlapped the oxide cut to the silicon by approximately 25 μm . An external p-type guard ring can also be seen in the figure; it is grounded in all the measurements. Irradiations were performed with +50V applied to the back contact with the front p^+ contact and guard ring grounded.



#4 FINGERS AL UNCOVER

Figure 5. The wafer design of test structures having variable edge-to-area ratios for gamma irradiation studies.

Figure 6 shows a typical result of increasing leakage current with irradiations of a 0.25cm^2 multiple (or "five") fingered detector up a total fluence of 1.84 Mrad. Depletion occurs at about 90V and one can see a relatively large increase in the first 150 Krad. The data are corrected for temperature and referred to 20C according to the relationship $T^2 \exp(0.65\text{eV}/kT)$ which well represents the $I(V,T)$ behavior of several control detectors [10,11] during neutron damage studies.

IV 302-14 SMALL FIVE GAMMA IRRADIATION

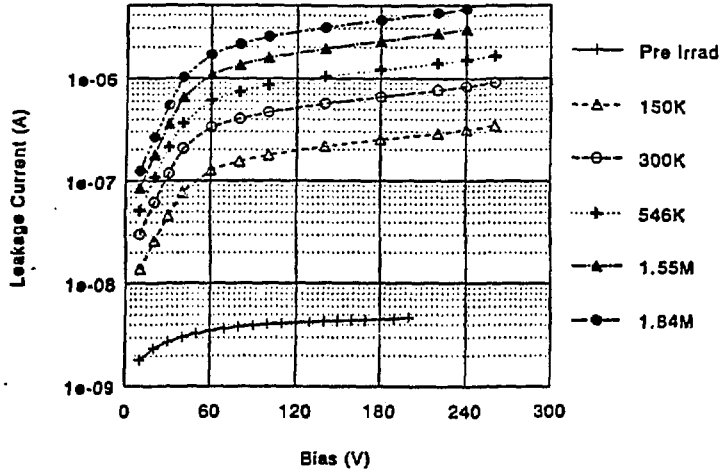


Figure 6. Typical effect of gamma dose to 1.84 Mrad on the leakage current of "5-fingered" small test structure.

The self annealing characteristics of each of a set of small area detectors with the perimeter to area ratios of 1,2 and 5 were observed to establish a $t=0$ reference(at the start of irradiation) and the results are shown in Table I. The leakage current is composed of components according to the summation:

$$I(t)/I(t=0) = \sum_i a_i \exp(-t/\tau_i) \quad \text{and} \quad \sum_i a_i = 1 \quad (1)$$

Table I

Leakage Current Annealing Fractions

Fraction (i) at $t=0$	Current at $t=0$ (μA) [Fraction]			Average Fraction a_i
	13 (single) x1	15 (3) x2	14 (5) x5	
1 $\tau_1 = 79.4 \pm 4$ min	2.58 [0.76]	6.7 [0.84]	11.5 [0.72]	0.78 ± 0.045
2 $\tau_2 = 3.95 \pm .08$ day	0.61 [0.24]	0.98 [0.123]	3.2 [0.204]	0.17 ± 0.03
3 $\tau_3 \approx 40$ day	0.2 [0.059]	0.3 [0.04]	1.0 [0.06]	0.053 ± 0.01
4 Constant (initial)	.002	0.002	0.002	-----
Total Leakage Current at $t=0$	3.39	7.98	15.7	

Figure 7 shows the increase of current just above depletion of the detectors having different edge to volume ratios (denoted as factors in parentheses following the detector number) as a function of increasing gamma fluence. Correction is again made to 20C and annealing is taken into account in the following way. The observed current is corrected by multiplying a factor called f^{-1} [12] and also described in much more detail in [13] where

$$f = \tau/T (1 - e^{-T/\tau}) e^{-t/\tau} \quad (2)$$

in which τ is the particular decay constant, essentially $\tau_2 = 3.95d$, T is the irradiation period and t is the elapsed time between the end of the irradiation and the measurement. For simplicity, measurements were made at least 24 hours after the irradiation to avoid the contribution of τ_1 and before a long term effect was evident. The contributions of each incremental irradiation were multiplied by the appropriate factor and a sum of the increments "weighted" by the incremental fluence to represent an uninterrupted irradiation.

LEAKAGE CURRENT vs GAMMA FLUENCE 0.25cm² Detectors (wafer 426)

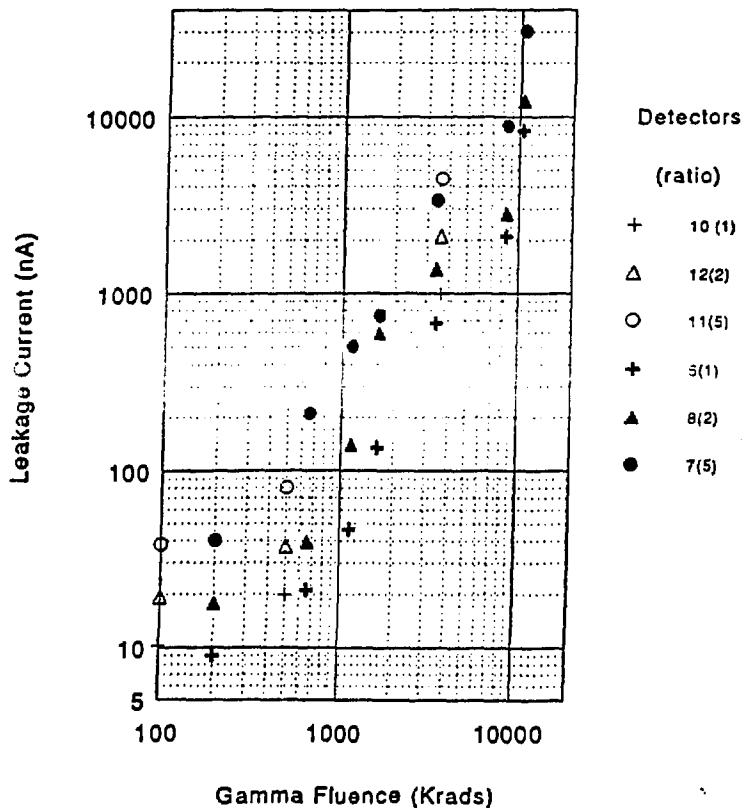


Figure 7. Increase in the Leakage Current versus Gamma Dose for several 0.25cm² detector shapes having 1x (6 and 10), 2x (8 and 12) and 5x (7 and 11) edge-to-area ratios.

Several comments can be made directly about the data in Figure 7. It is displayed on log-log axes and the data follow a power law with $n > 1$; clearly the increase in leakage current is greater than linear with fluence. An additional source of current beyond the generation component from mid-band interface states, directly proportional to fluence, would appear to be present. The data show considerable scatter which results in part from the difficulty in making simple, time independent measurements; some "charging effects" [13] were always present and patience is required to find a solid current value. Indeed, some I(V) curves similar to Figure 6 showed a reduction in current as bias was raised above the $-60V$ level; such effects may be appreciated following the simulation section. The ratios of current between detectors with 1, 2x and 5x the perimeter in general follows the perimeter ratios (as in the data points at 3400Krad) and a specifically good result is given in Table II for devices irradiated directly to 4.45Mrads.

Table II

Detector Leakage Currents after 4.45 Mrads

Small Detectors 426-() 0.25 cm ²	13 (single) x1	15 (3) x2	14 (5) x5
Leakage Current at Depletion, 20C μA	1.18	2.38	5.38
Ratio to Single x1	1.0	2.02	4.98
Current/cm ($\mu A/cm$)	0.59	0.595	0.588
Large Detectors 426-() 1.0 cm ²	01 (single) x1	09 (3) x2	03 (5) x5
Leakage Current at Depletion, 20C μA	2.89	5.06	12.9
Ratio to Single x1	1.0	1.75	4.46
Current/cm ($\mu A/cm$)	0.72	0.63	0.645

From the Table II data, one can derive a rate constant for the increase of leakage current per perimeter length per Mrad which lies in the range of 0.13 to 0.16 $\mu A/cm$ -Mrad. If the data of Figure 7 is expanded and limited to doses below 2 Mrad, a linear fit is easily made to the data from detector 426-7(5) and is 0.05 $\mu A/cm$ -Mrad. The change of slope between low and higher dose is obvious in Figure 7 and is not understood.

Figure 8 shows the capacitance vs. bias response of the simple small (.25cm²) square detector measured in the series mode at 100KHz after irradiation to 1.6 Mrad. The high capacity at low voltages is the capacitance of the metallization overlying the oxide adjacent to the junction to an extent of 25mm, which is estimated at 43pF for the perimeter contribution of the square detector. Larger perimeter capacitances are observed with the x2 and x5 perimeter detectors in agreement with this factor. This capacity senses the oxide charge initially and that induced by the radiation; a large flat band shift is caused by the initial 200 Krad which is not increased by further irradiation. The induced oxide charge that produced

this shift is calculated to be $2e12/cm^2$. In accord with the MOSCAP irradiations, the largest shift is the initial effect of only 200 Krad after which the total charge is balanced between that which is produced by irradiation and that which is lost by tunneling or rearrangement. Although the total oxide charge relaxes through increased irradiation, an increase in "stretchout" (10-90% of step) to $\sim 8V$ is observed indicating the increase of interface states at higher doses with lesser total charge. These observations are consistent with the view that oxide charge near the interface is subject to neutralization by the tunneling of electrons [14,15] from the bulk silicon especially as assisted by large electric fields at the interface due to the high accumulated positive charge and the accumulated electron density in the silicon.

An anomalous "bump" in the $C(V)$ curve is seen near depletion which affects the expected $1/V^{1/2}$ behavior; this bump is seen on the other higher perimeter ratio structures. If from the initial unirradiated capacitance curve, 2.5pF is simply subtracted from the higher bias values and in addition the 43pF of the perimeter capacitance is removed from the very low bias capacitance, a $C(V)$ response given by the filled circles in Figure 8 is derived which is very close to the full $1/V^{1/2}$ behavior. That the additional 2.5pF is mainly evident near depletion suggest that it may be a final "spreading" component near the rear contact, however its precise origin is as yet undetermined.

C(V) RESPONSE 426-6 SINGLE GAMMA IRRADIATION

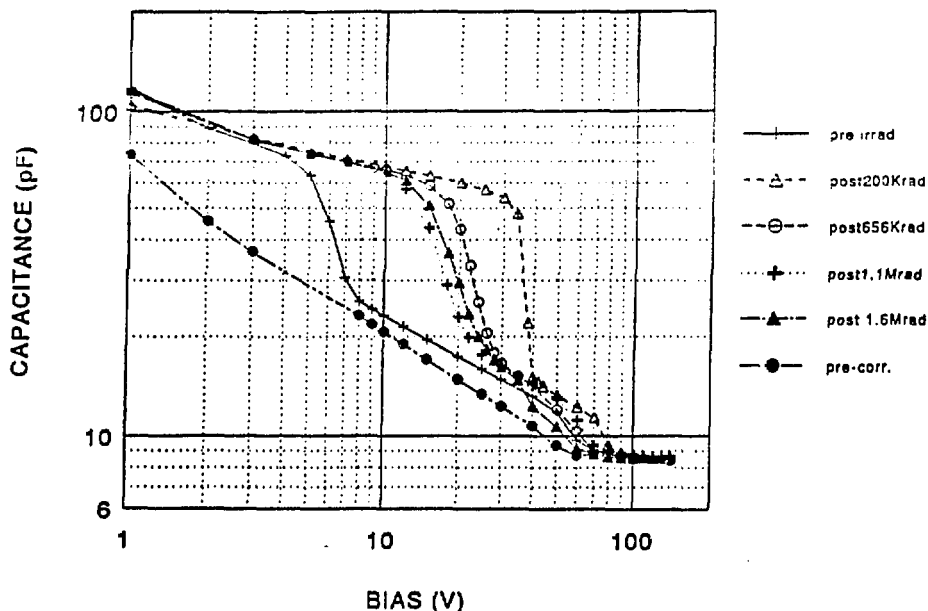


Figure 8. Capacitance versus Bias for $0.25cm^2$ "square" detector with a 1x edge-to-area ratio.

Simulation Studies

The simulation program SPICES [16] has been used to determine the electric field distribution at a typical junction edge with representative oxide thickness, metallization and surface charges. Figures 9 and 10 are examples of the potential distribution at the junction edge and electric fields in the x (lateral) and y (vertical) directions along a "cut line" running parallel to the oxide-silicon interface, 0.1 μm into the silicon from the interface. Figure 9 illustrates the case for $Q_{SS} = 5e11/\text{cm}^2$, which is a slightly elevated surface charge from the unirradiated junction and Figure 10 is the case for $Q_{SS} = 2e12/\text{cm}^2$, the fully irradiated value giving a V_{fb} of 20-30V. The electric potential is displayed on the left and is somewhat more demonstrative than a plot of the electric field components themselves in the areas where a very high electric field can be expected, clearly in the lateral direction near the junction. A significant vertical field is also shown which in fact increases approaching the interface. Figure 11 summarizes the maximum of the lateral electric fields for three surface charges as a function of applied bias to the detector as determined by the simulations. Clearly the simulations indicate a region near the junction edge having a very large electric field, comparable to fields that can generate "warm" if not hot carriers.

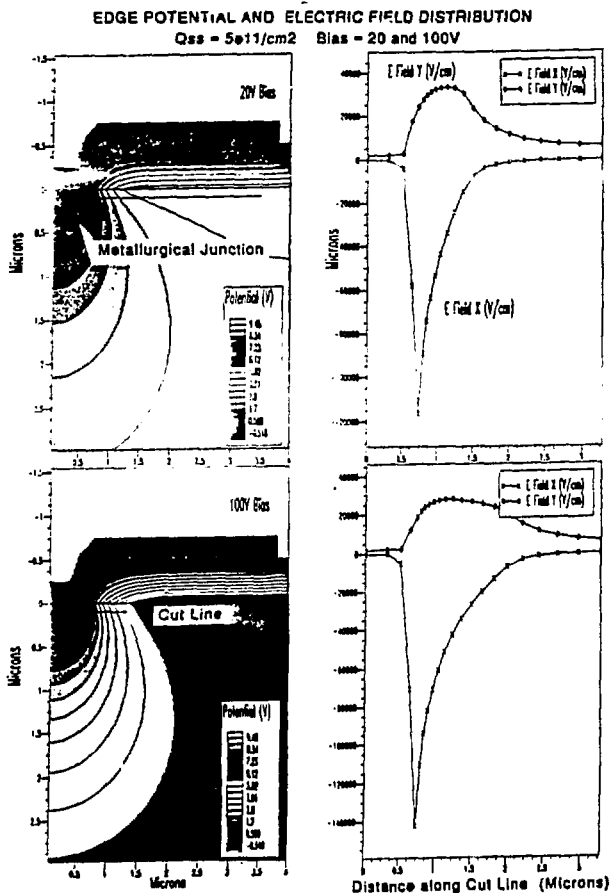


Figure 9. Simulated Edge Potential and Electric Field Distribution for junction with oxide surface charge of $5e11/\text{cm}^2$.

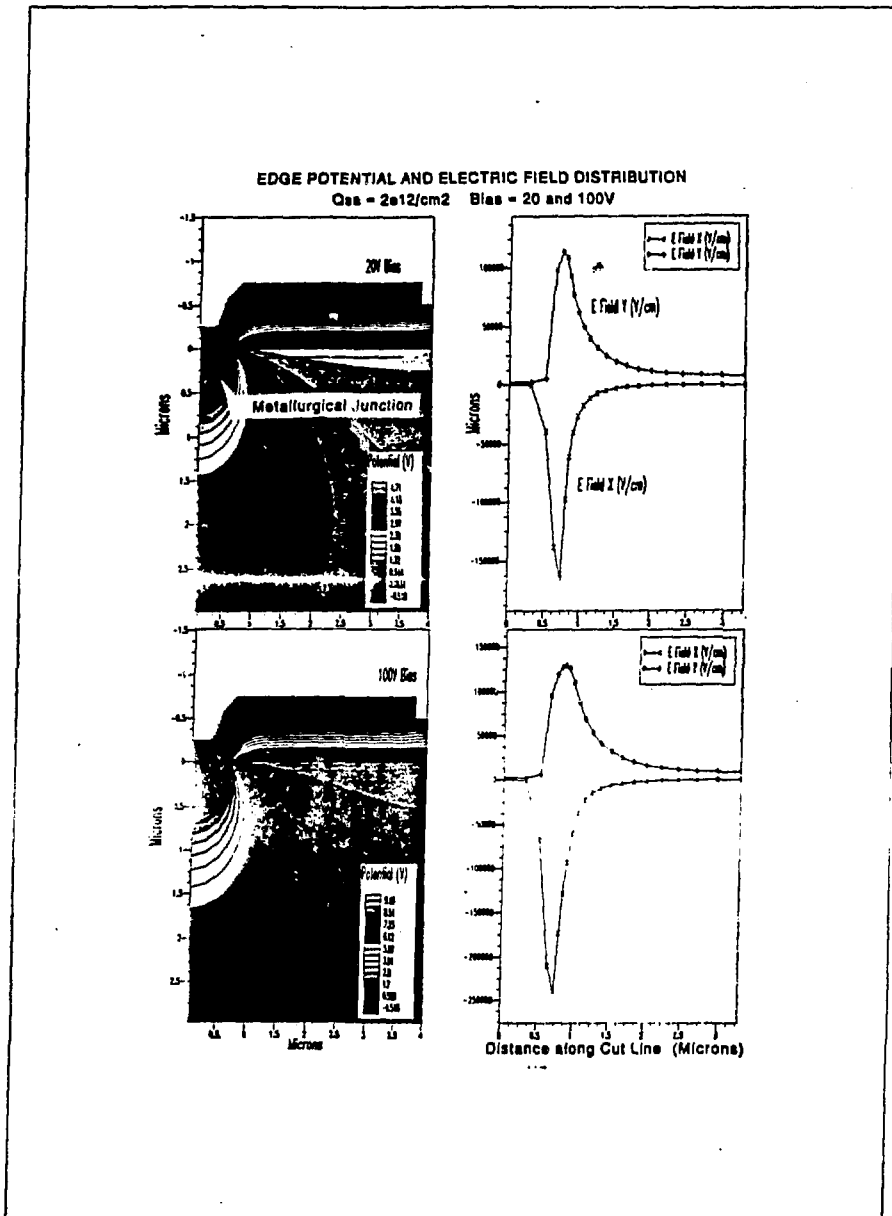


Figure 10. Simulated Edge Potential and Electric Field Distribution for junction with oxide surface charge of $2e12/cm^2$.

MOS CAPACITOR POTENTIAL
 $Q_{ss} = 2 \times 10^{12}/\text{cm}^2$ Bias = 30V

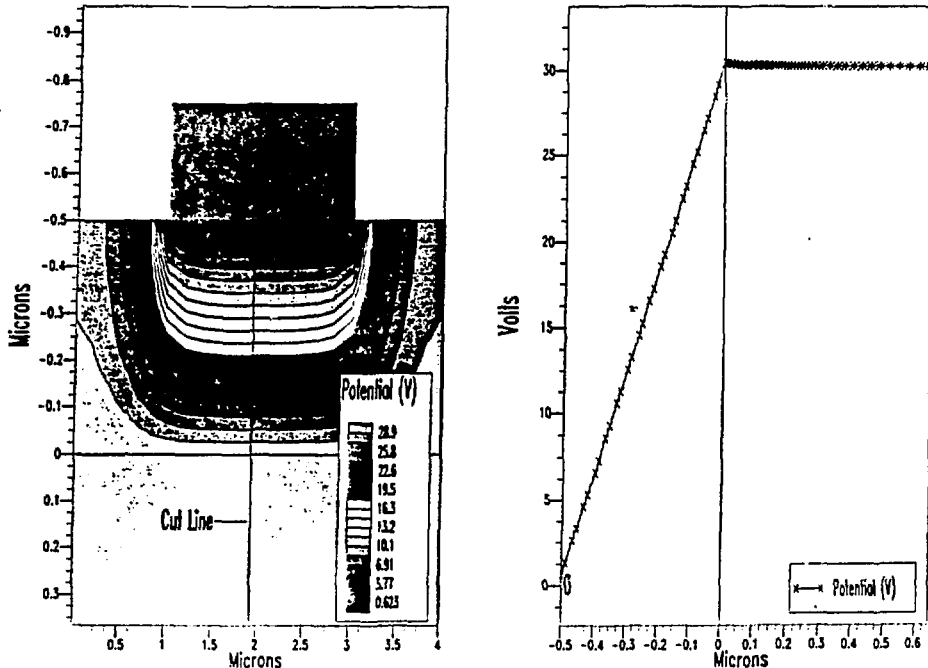


Figure 12. Electric Potential Distribution for a MOS Capacitor biased to 30V with a total oxide charge $Q_{ss} = 2 \times 10^{12}/\text{cm}^2$.

Discussions and Conclusions

It was instructive to begin this study with direct MOSCAP measurements on representative oxides and materials. Few surprises were found from the expected effects [1], however it is still impressive to measure the amount of accumulated positive charge from a relatively small dose (100Krad) if there is no avenue for decrease of this charge as there is in the case of the adjacent junction diode as illustrated in Figure 8. The simulation shown in Figure 12 indicates that little electrical field is present at the oxide-silicon interface to induce tunneling of electrons across the interface to neutralize the accumulated positive charge as evidenced by the very large flat band voltage shifts. To the contrary, in the region adjacent to the junction diodes, under the metallization, the simulations show a considerable vertical (E_y) electric field which must induce tunneling of electrons [14] and therefore charge neutralization that is obvious from the "saturation" of V_{fb} in Figure 8. The $\ln(t)$ behavior of the anneal of V_{fb} of MOSCAPs, is discussed in [9], [14] and [15] and involves both the reduction of trapped hole concentration by tunneling and filling effects of existing hole traps; it is not a simple issue. It is also observed that although the p^+n diode structures common in passivated position sensitive radiation detectors are biased to drive electrons not holes towards the Si-SiO_2 interface, a substantial increase in positive oxide charge and increase in V_{fb} is indeed observed. This case is not as deleterious as if the device were positively biased [3], however the increase in oxide positive charge may very well be fixed bulk charge and

not totally that associated with interface states; due to the mobility of electrons in SiO₂, it is subject to annealing from tunneled electrons in either case. However some "stretchout" of the C(V) characteristic is also evident in the negative bias cases, Figures 1 and 2 and that is the predominant effect in the unbiased irradiation from interface states formed by very local ionization before recombination occurs.

The special geometry of the test wafers permits the conclusion that the irradiation produced leakage current was due to effects at the junction edge and proportional to detector edge (Table II). Separate annealing parameters were established with a clear fast component (79 min) and moderate (3.95day) decay time component together with a longer component of the order of weeks. The increase in leakage current with dose apparently shows two components when plotted on a log log scale, Figure 7. A rate constant referred to anneal-corrected, several hours post irradiation currents for the higher dose range gives a value in the range of 0.13 to 0.16 $\mu\text{A}/\text{cm-Mrad}$ and a value of 0.05 $\mu\text{A}/\text{cm-Mrad}$ for doses below 2 Mrad. That the the current versus dose response is both slightly supra linear and suggests two ranges is not well understood at present, but some help may be found in the simulations.

Capacitance measurements (Figure 8) showed the expected effect of increased oxide charge under the overlaid metallization and in general agree with other reports [cf. 17]. The addition of an incremental 2.5pF that persists until full depletion must be attributed to a specific aspect of this fabrication procedure and as mentioned before may involve a final spreading effect at the rear contact at depletion. Taking this increment into account and the effect of increased oxide charge, a reasonable $1/V^{1/2}$ C(V) relationship is derived.

The SPICES simulations, Figures 9, 10 and 12 permitted the calculation of the lateral and vertical electric fields in the region of the Si-SiO₂ interface, which showed the effect of accumulation in producing very high electric fields, mostly laterally, in silicon very close to the interface. Breakdown or critical fields in silicon can be calculated [18] and have been theorized for several junction types [19]. Grove et al [20, and the bibliography therein] have considered the edge field breakdown problem in great detail. For 4000 Ωcm silicon, one finds a $E_{bd} \sim 1.3e5\text{V}/\text{cm}$ [18] which is certainly much less than the fields suggested by SPICES and one therefore expects a high current discharge condition to exist. However, prior to total breakdown, "soft spots" along the junction edge might be expected to exhibit higher leakage components (microplasmas, [21]) and be precursors to very high current discharge. Assuming that the surface charge may undergo some neutralization and rearrangement, the very high fields suggested by SPICES, Figure 11, are not necessarily expected, however there is every opportunity for a breakdown-like component of leakage current to exist. Such an addition might be expected to add non-linearly to the linear increase in current with gamma dose from the linear increase in interface generation state concentration. These effects would therefore cause a greater than linear increase in leakage current with gamma dose as observed.

Finally, it can be mentioned that the particular geometry of the test detectors offered an opportunity to observe a possible displacement damage component to the leakage current if it existed. From the results of Table II, no obvious component can be suggested; all the currents tend to be in the correct edge ratios. If one stretches the calculated displacement dose from Van Ginneken [22] to be 1.5e-6 keV/gm-cm² and uses a ratio to fast neutron effects, one would require $\gg 150\text{Mrad}$ for a leakage current as might be observed as in the case for even $1e^{11}\text{n}/\text{cm}^2$.

Acknowledgements

It is a pleasure to thank Dr. E. Heijne, CERN, for several helpful discussions and references.

Bibliography

1. T. P. Ma and P. V. Dressendorfer, "Ionizing Radiation Effects in MOS Devices and Circuits", John Wiley, NY (1989).
2. E. H. Nicollian and J. R. Brews, "MOS (Metal Oxide Semiconductor) Physics and Technology", John Wiley, NY (1982).
3. P. S. Winokur, J. M. McGarrity and H. E. Boesch Jr., "Interface Generation in Radiation-Hard Oxides", *IEEE Trans. Nucl. Sci.* **NS-23**, 1580 (1976).
4. Z. Li and H. W. Kraner, "Gettering in High Resistivity float Zone Silicon Wafers for Silicon Detector Applications", *IEEE TNS* **37**, 290, (1989).
5. K. Nauka, J. Lagowski and H. C. Gatos, and O. Ueda, "New Intrinsic Gettering Process in Silicon Based on Interaction of silicon Interstitials", *J. Appl. Phys.*, **60**, 615 (1986).
6. P. S. Winokur, J. M. McGarrity and H. E. Boesch Jr., "Dependence of Interface-State Buildup on Hole Transport in Irradiated MOS Capacitors", *IEEE Trans. Nucl. Sci.* **NS-23**, 1580 (1976).
7. K. O. Jeppson and C. M. Svensson. "Negative Bias Stress of MOS Devices at High Electric Fields and Degradation of MNOS Devices", *J. Appl. Phys.*, **48**, 2004 (1977).
8. G. J. Brucker, "Exposure-Dose-Rate-dependence for a CMOS/SOS Memory", *IEEE Trans. Nucl. Sci.* **NS-28**, 4056, (1981).
9. P. S. Winokur, K. G. Kerris and L. Harper, "Predicting CMOS Inverter Response in Nuclear and Space Environments", *IEEE Trans. Nucl. Sci.* **NS-30**, 4326(1983).
10. Separate study BNL (1993).
11. G. Lindstroem, "Radiation Damage in Silicon Detectors", SITP-Internal Note, University of Hamburg, Germany, Feb. 10, (1991).
12. Stuart Tovey, "On Self-Annealing Corrections", SITP-Note-029, CERN, March 31 (1992).
13. E. H. Nicollian, A. Goetzberger and C. N. Berglund, "Avalanche Injection Currents and Charging Phenomena in Thermal SiO₂", *Appl. Phys. Lett.* **15**, 174 (1969).
14. T. R. Oldham, A. J. Lelis and F. B. McClean, "Spatial Dependence of Trapped Holes Determined from Tunneling Analysis and Measured Annealing", *IEEE Trans. Nucl. Sci.* **NS-33**, 1203 (1986).

15. H. E. Boesch Jr., F. B. McLean, J. M. Benedetto and J. M. McGarrity, "Saturation of Threshold Voltage Shift in MOSFET's at High Total Dose", IEEE Trans. Nucl. Sci. NS-33, 1191 (1986).
16. S-PISCES 2B, Silvaco International Corp., 4701 Patrick Henry Dr., Bldg. 3, Santa Clara, CA 94054-1819.
17. D. S. Zoroglu and L. E. Clark, "Design Considerations for High Voltage Overlay Annular Diodes", IEEE Trans. Electron Devices, ED-19, 4 (1971).
18. S. K. Ghandi, "Semiconductor Power Devices", John Wiley & Sons NY (1977).
19. S. M. Sze and G. Gibbons, "Effect of Junction Curvature on Breakdown Voltage in Semiconductors", Solid State Electronics, 9, 831 (1966).
20. A. S. Grove, O. Leistiko, Jr. and W. W. Hooper, "Effect of Surface Fields on the Breakdown Voltage of Planar Silicon p-n Junctions", IEEE Trans. Electron Devices, ED-14, 157 (1967).
21. H. Kressel, "A Review of the Effect of Imperfections on the Electrical Breakdown of P-N Junctions", RCA Review, 28, 175 (1967).
22. A. Van Ginneken, Fermilab Note FN-522 (1989).